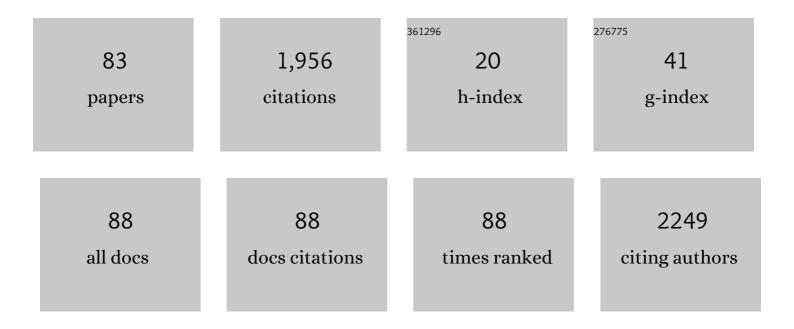
Laura J Olivieri

List of Publications by Year in descending order

Source: https://exaly.com/author-pdf/4207105/publications.pdf Version: 2024-02-01



ΙΛΠΟΛΙΟΠΝΙΕΡΙ

#	Article	IF	CITATIONS
1	Semi-Automatic Planning and Three-Dimensional Electrospinning of Patient-Specific Grafts for Fontan Surgery. IEEE Transactions on Biomedical Engineering, 2022, 69, 186-198.	2.5	9
2	Computational Modeling of Right Ventricular Motion and Intracardiac Flow in Repaired Tetralogy of Fallot. Cardiovascular Engineering and Technology, 2022, 13, 41-54.	0.7	13
3	Myocardial Parametric Mapping by Cardiac Magnetic Resonance Imaging in Pediatric Cardiology and Congenital Heart Disease. Circulation: Cardiovascular Imaging, 2022, 15, CIRCIMAGING120012242.	1.3	9
4	Computational Fontan Analysis: Preserving Accuracy While Expediting Workflow. World Journal for Pediatric & Congenital Heart Surgery, 2022, 13, 293-301.	0.3	4
5	Virtual Reality Cardiac Surgical Planning Software (CorFix) for Designing Patient-Specific Vascular Grafts: Development and Pilot Usability Study. JMIR Cardio, 2022, 6, e35488.	0.7	3
6	Aortic tortuosity in Turner syndrome is associated with larger ascending aorta. International Journal of Cardiovascular Imaging, 2022, 38, 2479-2490.	0.2	1
7	Aorta size mismatch predicts decreased exercise capacity in patients with successfully repaired coarctation of the aorta. Journal of Thoracic and Cardiovascular Surgery, 2021, 162, 183-192.e2.	0.4	9
8	Impact of incorporating echocardiographic screening into a clinical prediction model to optimise utilisation of echocardiography in primary care. International Journal of Clinical Practice, 2021, 75, e13686.	0.8	4
9	Magnetic Resonance Imaging–Guided Cardiac Catheterization Evacuation Drills. Critical Care Nurse, 2021, 41, e19-e26.	0.5	1
10	Combining patient-specific, digital 3D models with tele-education for adolescents with CHD. Cardiology in the Young, 2021, , 1-6.	0.4	1
11	Moving beyond size: vorticity and energy loss are correlated with right ventricular dysfunction and exercise intolerance in repaired Tetralogy of Fallot. Journal of Cardiovascular Magnetic Resonance, 2021, 23, 98.	1.6	13
12	Cardiac echocardiogram findings of severe acute respiratory syndrome coronavirus-2-associated multi-system inflammatory syndrome in children. Cardiology in the Young, 2021, , 1-9.	0.4	14
13	Altered hemodynamics by 4D flow cardiovascular magnetic resonance predict exercise intolerance in repaired coarctation of the aorta: an in vitro study. Journal of Cardiovascular Magnetic Resonance, 2021, 23, 99.	1.6	6
14	Society for Cardiovascular Magnetic Resonance 2020 Case of the Week series. Journal of Cardiovascular Magnetic Resonance, 2021, 23, 108.	1.6	7
15	Spontaneous rupture of a coronary artery fistula presenting with post-exertional syncope and haemopericardium. Interactive Cardiovascular and Thoracic Surgery, 2021, 32, 658-660.	0.5	1
16	Right ventricular afterload in repaired D-TGA is associated with inefficient flow patterns, rather than stenosis alone. International Journal of Cardiovascular Imaging, 2021, 38, 653.	0.7	1
17	Abstract 10071: Improved Accuracy of 4D Flow with Ferumoxytol in Comparison to Gadolinium Contrast for Small Children with Congenital Heart Disease. Circulation, 2021, 144, .	1.6	1
18	Ventricular arrhythmia risk prediction in repaired Tetralogy of Fallot using personalized computational cardiac models. Heart Rhythm, 2020, 17, 408-414.	0.3	35

#	Article	IF	CITATIONS
19	InÂvivo implantation of 3-dimensional printed customized branched tissue engineered vascular graft in a porcine model. Journal of Thoracic and Cardiovascular Surgery, 2020, 159, 1971-1981.e1.	0.4	25
20	3D Modeling as a Medical Education Resource, Simulation, and Communication Tool. , 2020, , 147-154.		1
21	Motion-corrected cardiac MRI is associated with decreased anesthesia exposure in children. Pediatric Radiology, 2020, 50, 1709-1716.	1.1	7
22	Automatic Shape Optimization of Patient-Specific Tissue Engineered Vascular Grafts for Aortic Coarctation. , 2020, 2020, 2319-2323.		9
23	Non-invasive Prediction of Peak Systolic Pressure Drop across Coarctation of Aorta using Computational Fluid Dynamics*. , 2020, 2020, 2295-2298.		5
24	Atrial fibrillation detection with a portable device during cardiovascular screening in primary care. Heart, 2020, 106, 1261-1266.	1.2	5
25	Troponin I Levels Correlate with Cardiac MR LGE and Native T1 Values in Duchenne Muscular Dystrophy Cardiomyopathy and Identify Early Disease Progression. Pediatric Cardiology, 2020, 41, 1173-1179.	0.6	14
26	4-Dimensional Flow by Cardiac Magnetic Resonance Informs Surgical Planning in Partial Anomalous Pulmonary Venous Return. JACC: Case Reports, 2020, 2, 672-677.	0.3	2
27	Quantitative cardiac magnetic resonance T2 imaging offers ability to non-invasively predict acute allograft rejection in children. Cardiology in the Young, 2020, 30, 852-859.	0.4	16
28	Normal right and left ventricular volumes prospectively obtained from cardiovascular magnetic resonance in awake, healthy, 0- 12 year old children. Journal of Cardiovascular Magnetic Resonance, 2020, 22, 11.	1.6	14
29	Role of surgeon intuition and computer-aided design in Fontan optimization: A computational fluid dynamics simulation study. Journal of Thoracic and Cardiovascular Surgery, 2020, 160, 203-212.e2.	0.4	23
30	Cardiac changes in pediatric cancer survivors. Journal of Investigative Medicine, 2020, 68, 1364-1369.	0.7	5
31	A Novel Virtual Reality Medical Image Display System for Group Discussions of Congenital Heart Disease: Development and Usability Testing. JMIR Cardio, 2020, 4, e20633.	0.7	21
32	CorFix: Virtual Reality Cardiac Surgical Planning System for Designing Patient Specific Vascular Grafts. , 2020, , .		4
33	Abstract 16727: Cardiac Complications of SARS CoV-2 Associated Multi-System Inflammatory Syndrome in Children (mis-c). Circulation, 2020, 142, .	1.6	0
34	Abstract 16754: Novel Characterization of Pulmonary Artery Bending, Rather Than Stenosis, Detects Increased Right Ventricular Afterload and is Associated With Increased Right Ventricular Mass in the Post-Arterial Switch Operation Heart. Circulation, 2020, 142, .	1.6	0
35	Improved Workflow for Quantification of Right Ventricular Volumes Using Free-Breathing Motion Corrected Cine Imaging. Pediatric Cardiology, 2019, 40, 79-88.	0.6	8
36	Abnormal Pulmonary Artery Bending Correlates With Increased Right Ventricular Afterload Following the Arterial Switch Operation. World Journal for Pediatric & Congenital Heart Surgery, 2019, 10, 572-581.	0.3	8

#	Article	IF	CITATIONS
37	Xâ€ray fused with MRI guidance of preâ€selected transcatheter congenital heart disease interventions. Catheterization and Cardiovascular Interventions, 2019, 94, 399-408.	0.7	9
38	Computational Study of Pulmonary Flow Patterns After Repair of Transposition of Great Arteries. Journal of Biomechanical Engineering, 2019, 141, .	0.6	9
39	Design and Simulation of Patient-Specific Tissue-Engineered Bifurcated Right Ventricle-Pulmonary Artery Grafts using Computational Fluid Dynamics. , 2019, , .		2
40	Anesthetic considerations for magnetic resonance imagingâ€guided rightâ€heart catheterization in pediatric patients: A single institution experience. Paediatric Anaesthesia, 2019, 29, 8-15.	0.6	17
41	Validation of cardiac magnetic-resonance-derived left ventricular strain measurements from free-breathing motion-corrected cine imaging. Pediatric Radiology, 2019, 49, 68-75.	1.1	2
42	Virtual Cardiac Surgical Planning Through Hemodynamics Simulation and Design Optimization of Fontan Grafts. Lecture Notes in Computer Science, 2019, , 200-208.	1.0	5
43	Virtual surgical planning, flow simulation, and 3-dimensional electrospinning of patient-specific grafts to optimize Fontan hemodynamics. Journal of Thoracic and Cardiovascular Surgery, 2018, 155, 1734-1742.	0.4	41
44	Novel, 3D Display of Heart Models in the Postoperative Care Setting Improves CICU Caregiver Confidence. World Journal for Pediatric & Congenital Heart Surgery, 2018, 9, 206-213.	0.3	17
45	Respiratory variation in peak aortic velocity accurately predicts fluid responsiveness in children undergoing neurosurgery under general anesthesia. Journal of Clinical Monitoring and Computing, 2018, 32, 221-226.	0.7	19
46	Myocardial Strain Using Cardiac MR Feature Tracking and Speckle Tracking Echocardiography in Duchenne Muscular Dystrophy Patients. Pediatric Cardiology, 2018, 39, 478-483.	0.6	22
47	Junctional ectopic tachycardia secondary to myocarditis associated with sudden cardiac arrest. HeartRhythm Case Reports, 2017, 3, 124-128.	0.2	10
48	Feasibility of low radiation dose retrospectively-gated cardiac CT for functional analysis in adult congenital heart disease. International Journal of Cardiology, 2017, 228, 180-183.	0.8	19
49	Acute Cardiac MRI Assessment of Radiofrequency Ablation Lesions for Pediatric Ventricular Arrhythmia: Feasibility and Clinical Correlation. Journal of Cardiovascular Electrophysiology, 2017, 28, 517-522.	0.8	14
50	The Role of 3-D Heart Models in Planning and Executing Interventional Procedures. Canadian Journal of Cardiology, 2017, 33, 1074-1081.	0.8	20
51	Usage of 3D models of tetralogy of Fallot for medical education: impact on learning congenital heart disease. BMC Medical Education, 2017, 17, 54.	1.0	134
52	Virtual Surgery for Conduit Reconstruction of the Right Ventricular Outflow Tract. World Journal for Pediatric & Congenital Heart Surgery, 2017, 8, 391-393.	0.3	14
53	VALIDATION OF CMR-DERIVED LEFT VENTRICULAR STRAIN MEASUREMENTS BY FREE-BREATHING MOTION-CORRECTED CINE IMAGING. Journal of the American College of Cardiology, 2017, 69, 1448.	1.2	1
54	Impact of Three-Dimensional Printing on the Study and Treatment of Congenital Heart Disease. Circulation Research, 2017, 120, 904-907.	2.0	53

#	Article	IF	CITATIONS
55	Septal Defects. , 2017, , 63-68.		Ο
56	Dark blood Late Gadolinium Enhancement improves conspicuity of ablation lesions. Journal of Cardiovascular Magnetic Resonance, 2016, 18, P211.	1.6	8
57	Novel Uses for Three-Dimensional Printing in Congenital Heart Disease. Current Pediatrics Reports, 2016, 4, 28-34.	1.7	15
58	Ductal constriction during dexamethasone treatment in an anti-SSA-antibody-exposed fetus with signs of myocardial inflammation. Cardiology in the Young, 2016, 26, 1021-1024.	0.4	2
59	Improved workflow for quantification of left ventricular volumes and mass using free-breathing motion corrected cine imaging. Journal of Cardiovascular Magnetic Resonance, 2016, 18, 10.	1.6	24
60	White Paper on P4 Concepts for Pediatric Imaging. Journal of the American College of Radiology, 2016, 13, 590-597.e2.	0.9	11
61	Free-breathing motion-corrected late-gadolinium-enhancement imaging improves image quality in children. Pediatric Radiology, 2016, 46, 983-990.	1.1	20
62	"Just-In-Time―Simulation Training Using 3-D Printed Cardiac Models After Congenital Cardiac Surgery. World Journal for Pediatric & Congenital Heart Surgery, 2016, 7, 164-168.	0.3	77
63	Native T1 values identify myocardial changes and stratify disease severity in patients with Duchenne muscular dystrophy. Journal of Cardiovascular Magnetic Resonance, 2016, 18, 72.	1.6	51
64	Dark blood late enhancement imaging. Journal of Cardiovascular Magnetic Resonance, 2016, 18, 77.	1.6	64
65	Radiation-free CMR diagnostic heart catheterization in children. Journal of Cardiovascular Magnetic Resonance, 2016, 19, 65.	1.6	45
66	Incorporating Three-dimensional Printing into a Simulation-based Congenital Heart Disease and Critical Care Training Curriculum for Resident Physicians. Congenital Heart Disease, 2015, 10, 185-190.	0.0	179
67	Congenital Aneurysm of the Aortomitral Intervalvular Fibrosa. Annals of Thoracic Surgery, 2015, 99, 314-316.	0.7	9
68	Three-Dimensional Printing of Intracardiac Defects from Three-Dimensional Echocardiographic Images: Feasibility and Relative Accuracy. Journal of the American Society of Echocardiography, 2015, 28, 392-397.	1.2	164
69	Risk assessment and anesthetic management of patients with Williams syndrome: a comprehensive review. Paediatric Anaesthesia, 2015, 25, 1207-1215.	0.6	64
70	Palliation of Truncus Arteriosus Associated With Complete Atrioventricular Canal—Results of Single Ventricle Palliation. World Journal for Pediatric & Congenital Heart Surgery, 2015, 6, 663-666.	0.3	3
71	Optimized protocols for cardiac magnetic resonance imaging in patients with thoracic metallic implants. Pediatric Radiology, 2015, 45, 1455-1464.	1.1	18
72	Image Fusion Guided Device Closure of Left Ventricle to Right Atrium Shunt. Circulation, 2015, 132, 1366-1367.	1.6	6

#	Article	IF	CITATIONS
73	Acute endocarditis of a percutaneously placed pulmonary valve. Annals of Pediatric Cardiology, 2015, 8, 225.	0.2	1
74	Method for calculating confidence intervals for phase contrast flow measurements. Journal of Cardiovascular Magnetic Resonance, 2014, 16, 46.	1.6	4
75	Utilizing Three-Dimensional Printing Technology to Assess the Feasibility of High-Fidelity Synthetic Ventricular Septal Defect Models for Simulation in Medical Education. World Journal for Pediatric & Congenital Heart Surgery, 2014, 5, 421-426.	0.3	144
76	3D heart model guides complex stent angioplasty of pulmonary venous baffle obstruction in a Mustard repair of D-TGA. International Journal of Cardiology, 2014, 172, e297-e298.	0.8	83
77	Bicuspid aortic valve and aortic coarctation are linked to deletion of the X chromosome short arm in Turner syndrome. Journal of Medical Genetics, 2013, 50, 662-665.	1.5	78
78	Spectrum of Aortic Valve Abnormalities Associated With Aortic Dilation Across Age Groups in Turner Syndrome. Circulation: Cardiovascular Imaging, 2013, 6, 1018-1023.	1.3	42
79	Influence of Fetal Diagnosis on the Clinical Presentation of a Vascular Ring. Pediatric Cardiology, 2012, 33, 351-353.	0.6	3
80	Hypoplastic Left Heart Syndrome With Intact Atrial Septum. Journal of the American College of Cardiology, 2011, 57, e369.	1.2	11
81	Hemodynamic Modeling of Surgically Repaired Coarctation of the Aorta. Cardiovascular Engineering and Technology, 2011, 2, 288-295.	0.7	44
82	Coronary Artery Z Score Regression Equations and Calculators Derived From a Large Heterogeneous Population of Children Undergoing Echocardiography. Journal of the American Society of Echocardiography, 2009, 22, 159-164.	1.2	75
83	Abnormal Diastolic Hemodynamic Forces: A Link Between Right Ventricular Wall Motion, Intracardiac Flow, and Pulmonary Regurgitation in Repaired Tetralogy of Fallot. Frontiers in Cardiovascular Medicine, 0, 9, .	1.1	4